



**13<sup>TH</sup> CANADIAN MASONRY SYMPOSIUM**  
**HALIFAX, CANADA**  
**JUNE 4<sup>TH</sup> – JUNE 7<sup>TH</sup> 2017**



---

**EXPERIMENTAL STUDY ON TEXTILE REINFORCED MASONRY WALLS  
SUBJECTED TO LATERAL LOADING**

**Saenger, Dorothea<sup>1</sup> and Raupach, Michael<sup>2</sup>**

**ABSTRACT**

An innovative way to increase the load-bearing capacity of masonry building elements subjected to lateral loading caused by wind or earth pressure is to apply textile reinforcement embedded in mortar on the masonry surface. In order to better understand the performance of various types of textile reinforcement (alkali-resistant glass/carbon fiber) and mortar (cement render) as well as to evaluate their suitability for structural strengthening of masonry, an extensive experimental study is currently being carried out. The main objectives of this study are to find suitable reinforcing materials for the use on masonry as well as to describe the load-bearing and deformation behavior of textile reinforced masonry building elements and hence to derive a design model. This study includes tests on small scale composite specimens subjected to tensile, shear or bending loading, from which the required material and bond parameters for developing a design model can be defined. From large scale tests on masonry walls subjected to lateral loading, the effectiveness of strengthening masonry with textiles has been assessed. This paper describes the tests performed and presents the results and conclusions obtained so far.

**KEYWORDS:** *bond performance, flexural strength, lateral loading, reinforced masonry, tensile strength, textile reinforcement*

**INTRODUCTION**

Lateral loading on masonry constructions caused by earth pressure or wind can generate high out-of-plane shear, flexural and thus tensile stresses on masonry. However, the flexural tensile and particularly the tensile strength of unreinforced masonry are low, so that the fail-free recordable lateral loading is anyway limited.

---

<sup>1</sup> Masonry Research Engineer, Dipl.-Ing., RWTH Aachen University, Institute of Building Materials Research, 52062 Aachen, Germany, saenger@ibac.rwth-aachen.de

<sup>2</sup> Professor and Head of Institute, Dr.-Ing., RWTH Aachen University, Institute of Building Materials Research, 52062 Aachen, Germany, raupach@ibac.rwth-aachen.de

An innovative way to increase the load-bearing capacity of masonry building elements subjected to such stresses is to reinforce them with technical textiles. This idea arises from the knowledges gained in the past 20 years of investigations on textile reinforced concrete (TRC) and aims to take advantage of the benefits offered by technical textiles as reinforcement in comparison to steel [1]. In the case of masonry, the textile reinforcement can be embedded in the mortar bed joint in even thin-bed masonry. Additionally, it can be applied externally embedded in cement-based materials on the masonry surface. The external application is suitable not only for new structures, but also for the repair or strengthening of existing masonry buildings [2].

The experimental study presented below focused on the reinforcement of masonry structures with externally in cement render applied technical textiles. The main objectives of this study are to analyze the load-bearing and deformation behavior of such structures under flexural load and assess the reinforcement effectiveness especially for improving the masonry lateral load resistance. A higher flexural load resistance of textile reinforced masonry can only be ensured if the bond performance between the composite materials is high enough to transmit the tensile stresses acting on masonry to the textile reinforced rendering. Therefore, the first goal of this experimental study was to find suitable technical textiles to use in combination with the surrounding materials – render and masonry – based on the bond performance among each other under tensile stress. In addition, the bond performance between textile reinforced mortar (TRM) and masonry under shear and flexural load will be investigated. The second goal of this study was to assess the effectiveness of selected suitable materials for masonry reinforcing. For this purpose, flexural tensile tests on clay masonry walls with and without externally bonded reinforcement have been conducted.

## MATERIALS

In a preliminary study presented in [3] some combinations of mortars and alkali-resistant (AR) textiles with and without impregnation were tested in order to find suitable matching materials apart from calibrating the test method for the uniaxial tensile tests limited until then to TRC. Based on this a not impregnated AR-glass textile (T1) was selected for the investigations described below. In addition, an epoxy impregnated carbon textile (C1) was chosen for these investigations. Both textiles are shown in Figure 1. The characteristic properties of each of them are given in Table 1.

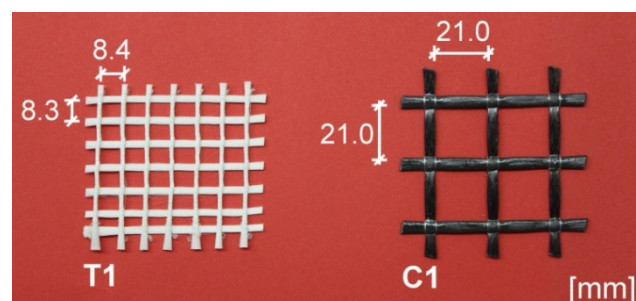


**Figure 1: AR-glass textile T1 and carbon textile C1**

**Table 1: Textile properties (mean values)**

label	material	impregnation	yarn fineness*	yarn cross- section area*		yarn tensile strength	
				0°	90°	0°	90°
			tex	mm <sup>2</sup> /m		MPa	
T1	AR glass	-	2400	105	105	1188	1077
C1	carbon	epoxy resin	3200	85	85	3300*	3550*

\*manufacturer specifications

As cementitious matrix two commercial renders (R1 and R2) were used for the investigations. Both of them are cement-based mixtures with the difference that R2 contains additionally additives in order to repel water. To characterize the material properties given in Table 2, the standard parameters (dry bulk density  $\rho_{d,m}$ , compressive strength  $f_{c,m}$  and flexural tensile strength  $f_{fl,m}$ ) were determined on each mixture according to the European standards EN 1015-10 and EN 1015-11. Differing from the stated storage climate, the demolded mortar prisms were stored in water at room temperature (20 °C) during curing analogous to the storing conditions of the bonding specimens for the uniaxial tensile tests. This may be the reason for the lower compressive strength obtained with R1 (6.9 MPa) compared to the declared one by the manufacturer ( $\geq 10$  MPa).

**Table 2: Mortar and render properties (mean values)**

label	type	compressive strength class*	grain size	$\rho_{d,m}$	$f_{c,m}$	$f_{fl,m}$
			mm	kg/dm <sup>3</sup>	MPa	MPa
G2	general purpose mortar	M5 ( $\geq 5$ MPa)	0-4	1.78	6.4	2.6
R1	render	CS IV ( $\geq 10$ MPa)	0-1.2	1.55	6.9	1.8
R2	render	CS III ( $\geq 5$ MPa)	0-1.2	1.61	5.6	1.9

\* manufacturer specifications according to EN 998-1 or EN 998-2

The masonry walls consisted of solid masonry clay units (U1) and a general purpose mortar (G2). The mortar properties determined according to EN 1015-10 and EN 1015-11 are given in Table 2. Table 3 contains the standard unit properties (length  $l$ , width  $w$  and height  $h$ , dry bulk density  $\rho_{d,u}$  and compressive strength in the direction of the unit height  $f_b$ ) determined according to EN 772-13 and EN 772-1. Further relevant properties (compressive strength  $f_{b,II}$ , tensile strength  $f_{t,u}$  and flexural tensile strength  $f_{fl}$  in the direction of the unit length) contained in Table 3 are needed to evaluate the unit behavior when bending the wall. The compressive and tensile strength were determined on solid masonry units as illustrated in Figure 2. The axial displacements were measured in each of the tests with linear variable displacement transducers (LVDT). The tensile load introduction was made by steel plates glued onto the masonry units and flexibly joined to the testing machine. The flexural strength was investigated on small test specimens under deformation-controlled 3-point bending tests, cf. Figure 2. The test specimens consisted of 5 solid masonry units connected by glue to lengthen the unit artificially and hence obtain a sufficient slenderness of the test specimens ( $\lambda = 5$ ). At these tests a compensation for the

specimen's dead weight was made. The deflection was measured with LVDTs in the middle of the specimen.

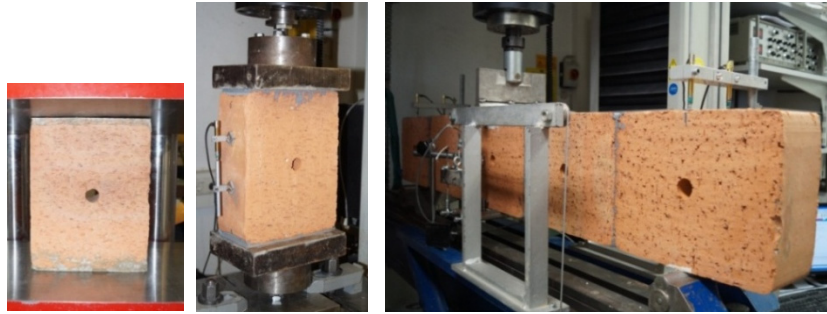


**Figure 2: Compression, tension and bending tests on masonry clay units in the direction of the unit length**

**Table 3: Masonry unit properties (mean values)**

label	material	l	w	h	$\rho_{d,u}$	$f_{b,u}$	$f_{b,II,u}$	$f_{t,u}$	$f_{fl,u}$
		mm	mm	mm	kg/dm <sup>3</sup>	MPa	MPa	MPa	MPa
U1	clay	306	243	115	1,79	21.8	9.3	0.3	0.7

### UNIAXIAL TENSILE TESTS ON TEXTILE REINFORCED RENDERING SPECIMENS

In order to determine the load-bearing behavior of composite specimens made of TRM, uniaxial tensile tests were conducted according to the recommendations of RILEM TC 232-TDT for TRC [4]. These recommendations include two test methods. One of them was developed by Scholzen et al. [5] especially for specimens with yarns exhibiting low bond to the matrix. Since in preliminary investigations on TRM described in [2] and [3], AR-glass textile showed a low bond/interlocking to the mortar matrix, this testing method was implemented here (cf. Figure 4).

A total of six series with each six specimens were produced and tested until now. The parameters varied in each series – like the material combination, the orientation of the textile in load direction as well as the specimen width and thickness – are given in Table 4.

The mortar specimens consisted of two layers of render and one layer of textile located in between. The specimen geometry and dimensions are presented in Figure 3, left. The specimen length was always 1000 mm in order to realize an anchorage length of 375 mm on both sides. The specimen width was 60 mm or 120 mm – depending on the mesh width of the embedded textile – to test not less than 5 yarns in test direction. The specimen thickness was 10 mm or 20 mm to cover even thicker yarns sufficiently with render. In view of the wall tests it was also important to find out which of these two thicknesses could be better for the reinforcing layer.

To cast the specimens, a hand-lamination process was used. Within a steel formwork, first a thin rendering layer was applied covering just about half of the formwork height. Then the textile was placed over this rendering layer, pressed into it and finally covered with a second thin rendering

layer (cf. Figure 3, right). Depending on the test series, the weft (90°) or warp (0°) direction of the textile was placed along the length of the specimen (cf. Table 4).

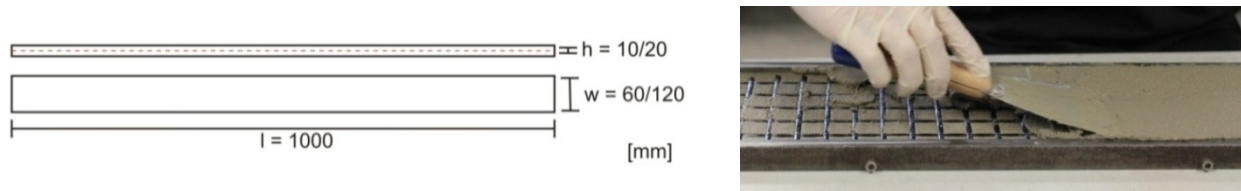


**Figure 3: Specimen geometry (left) and hand-lamination process (right)**

Once produced the specimens, they were stored in a humid environment (20 °C/95 % rel. humidity), demolded after 2 days and stored in water. One day before testing, they were removed from water and stored in laboratory climate (20 °C/65 % rel. humidity). Finally, they were tested at the age of 28 days.

The test set-up built for the uniaxial tensile tests is illustrated in Figure 4. Through longitudinal bars fixing the position of the stiff steel plates among the specimen, this test set-up allows increasing the anchorage length of the specimen and hence of the textile without being necessary to enlarge the clamping length. For these tests the maximum adjustable anchorage length of 375 mm was chosen. The clamping length remained constant with a value of 200 mm. The measuring length was 200 mm. The clamping pressure was applied by means of hydraulic pumps, allowing a controlled and homogeneous application. It was set equal to 2 MPa for all the tests.

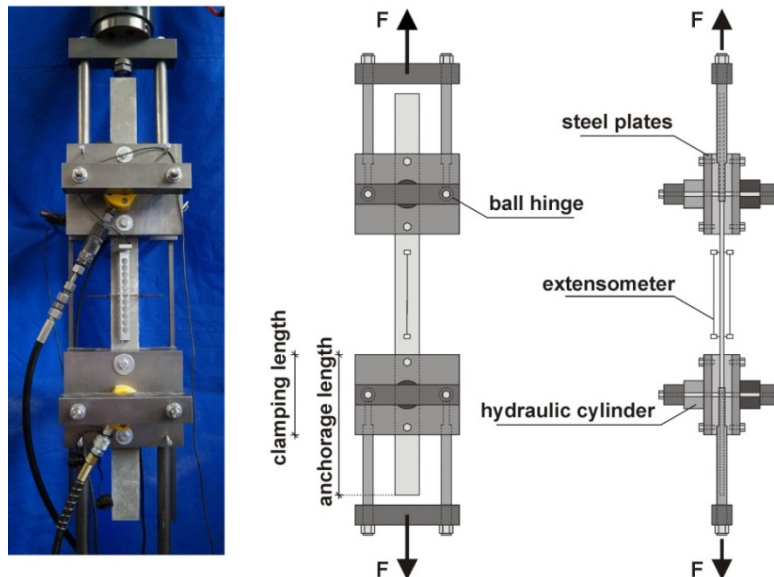


**Figure 4: Test set-up with variable textile anchorage length and fixed clamping length, hydraulic specimen clamping**

The uniaxial tensile tests were carried out in a displacement controlled way with a rate of 0.5 mm/min. The load was measured with standard load cells and the deformations were recorded by compact strain transducers attached on both surfaces in the middle of the specimen. The hydraulic clamping pressure applied was also recorded during the test.

As part of the analysis, the stress-strain curves of the TRM specimens were determined for each single tensile test and then evaluated with respect to the main influencing parameters tested. To obtain the tensile stress, the measured tensile load was related either to the composite specimen cross-section area ( $\sigma_m$ ) or to the textile cross-section area contained in the specimen ( $\sigma_t$ ). The longitudinal strain  $\varepsilon$  of the tensile specimen was determined by averaging the measured deformation of the strain transducers and then relating to the measuring length. In addition, the maximum tensile stress  $\sigma_{t,max}$  was related to the yarn tensile strength (cf. Table 1) to calculate the utilization degree of the textile  $\alpha_t$ . These values are given in Table 4. Moreover, the failure mode and the crack pattern were documented for each single test in order to better understand the results.

**Table 4: Uniaxial tensile tests: series and results**

ID no.	mortar	textile	test direction	w	h	$\sigma_{t,max}$		$\alpha_t$	
						min	max	min	max
						MPa		%	
26	R1	T1	0°	60	10	357	535	30	45
25	R2	T1	0°	60	10	275	405	23	34
32	R1	C1	0	120	20	2267	2696	69	82
34	R1	C1	90°	120	20	2223	2658	63	75
31	R2	C1	0°	120	10	1944	2293	59	70
33	R2	C1	0°	120	20	1991	2235	60	68

Figures 5 and 6 present the stress-strain curves obtained by testing specimens reinforced with AR-glass or carbon textile combined with the renders R1 and R2, respectively. In analogy with TRC, the strain-stress curves of TRM can be divided in three stages, depending on the composite specimen part – mortar and/or textile – being activated under load until it fails. These stages are: (1) uncracked mortar (2) multiple cracking and (3) complete cracking.

Since the renders R1 and R2 have similar mechanical properties (cf. Table 2), the differences between the stress-strain curves obtained with these renders in combination with one or the other textile are small (see Figure 5 and 6). Due to the low strength of the renders the first crack stress reached is in all cases smaller than 1.0 MPa. With respect to the textiles, the differences between the stress-strain curves of Figure 5 and 6 are clearly evident especially in the last part of the curves, when the cracking formation is completed (cf. Figure 5 with 6). The different material properties and geometry of the textiles as well as the impregnation influenced the bond performance between reinforcement and render and thus the crack formation up to the maximum achievable tensile strength. In the case of the not impregnated AR-glass textile T1, only the outer filaments of the yarns were interlocked with the render and a pull-out of the inner filaments of

the yarns occurred. The lack of impregnation, the textile structure as well as a presumably insufficient anchorage length of T1 favored this bond failure between textile and render, as would also have occurred with concrete with poor yarn interlocking. Especially the arc-shaped course at the end of the stress-strain curves of the specimens with T1 and R2 shown in Figure 5 denotes clearly this failure form. In the case of the impregnated carbon textile C1, the bond performance was much better, so that the tensile load could be transmitted to the textile. For this reason, after cracking formation was completed, the tensile stress grew linearly until textile failure was achieved (cf. (3) in Figure 6). The utilization degree of C1 (60-80 %) is therefore significantly higher than T1 (23-45 %) (cf. Table 4).

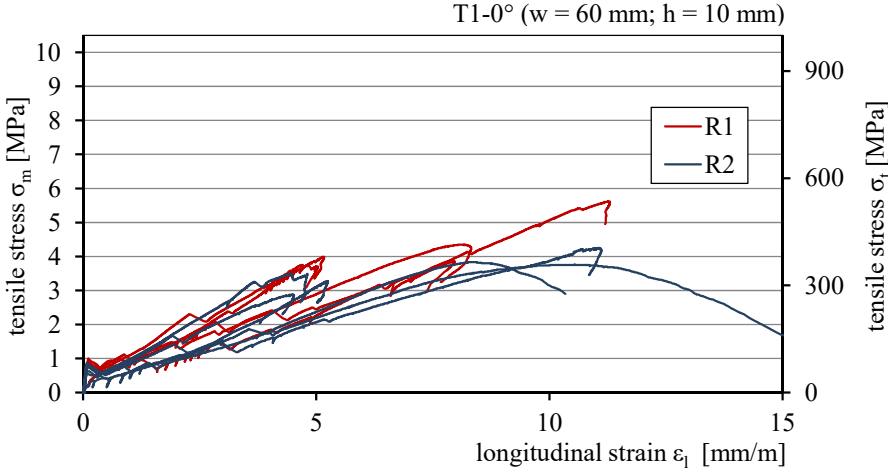


**Figure 5: Stress-strain curves of the specimens with AR-glass textile under tensile load**

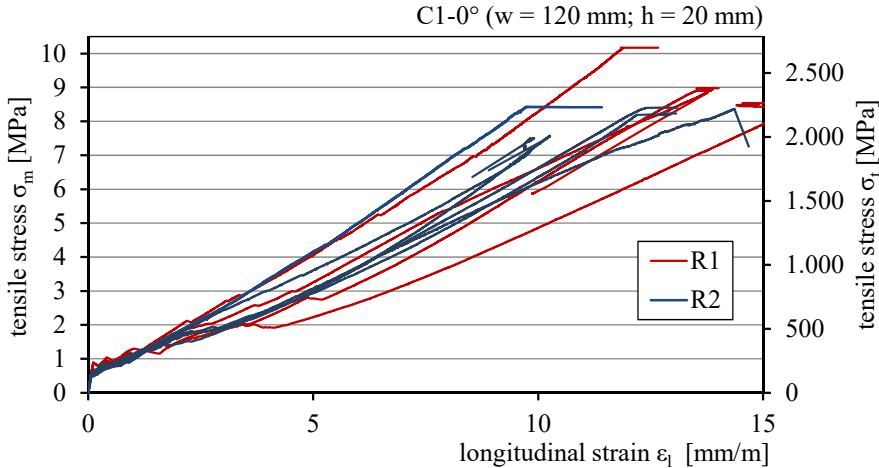


**Figure 6: Stress-strain curves of the specimens with carbon textile under tensile load**

A comparison of the thicknesses of the specimens with carbon textile was omitted here, since the differences in the results were negligibly small.

## **FLEXURAL TESTS ON MASONRY WALLS**

To assess the effectiveness of textile reinforced mortar especially for improving the masonry lateral load resistance, comparative flexural tests were performed on reinforced and unreinforced masonry walls. So far, only one of the two principal axes of loading was tested, namely parallel to the bed joint, which means for a failure plane perpendicular to the bed joints. Table 5 shows a survey of the conducted tests. In total, two series with each three walls were prepared and tested at an age of at least 28 days after completing the preparation of the specimens.

All the wall specimens were built using the clay units U1 and the general purpose mortar G2 for the bed joint. This material combination was selected due to its expected relatively low bonding strength and high unit tensile strength, so that the wall subjected to flexural loading would predominantly fail in the bond between unit and mortar. The head joints were not filled to allow a higher wall deformation and to cover the worst case with respect to the load transmission in the unit layer. The length of the wall specimens was 2.55 m and the height 1 m. The overlap of the units amounted 145 mm (half the unit length). Figure 7 exemplarily illustrates one of the unreinforced masonry wall specimens.

In the case of the reinforced masonry wall specimens, the reinforcing layer was applied five days after preparing the specimens in hand-lamination on one surface side with a total thickness of 20 mm as shown in Figure 8. The application was carried out in four steps: First the primer recommended by the render producer was applied on the wall surface, to avoid the clay units from absorbing too much water by coming in contact with the render. One day after, the treated masonry surface was covered with a rendering layer. Then the textile reinforcement was placed on the fresh rendering layer and covered with a second rendering layer. The materials used for reinforcing the wall were the render R1 and the carbon textile C1. These materials were chosen based on the results of the uniaxial tensile test, which confirmed a better bond performance of the carbon textile regardless of the render type used.



**Figure 7: Unreinforced masonry wall specimens**



**Figure 8: Textile reinforced rendering applied on one masonry wall side**

The flexural tests parallel to the bed joints were conducted according to EN 1052-2 on masonry walls. The principle of this test consists of a bending device in which the test wall is clamped between two outer bearings and is loaded by two inner bearings, as it corresponds to a four-point bending test. Figure 9 shows the pressure side of the bending device. Details about the wall dimension as well as the distance between inner and outer bearings are given in Figure 10.

Differing from the standard testing procedure, the load was applied in a displacement-controlled way with a rate of 0.5 mm/min in order to be able to determine the failure behavior beyond the flexural masonry strength of the reinforced masonry walls. During testing the deflection in the center of the wall was measured with respect to the outer bearings (see LVDT 1 and 2 in Figure 10). Furthermore comprehensive longitudinal deformation measurements were carried out on the tension side (cf. Figure 12).



**Figure 9: Test set-up with built-in wall under four-point bending**

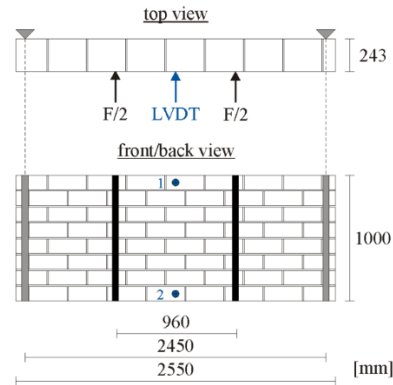


**Figure 10: Wall specimen geometry and static system**

Figure 11 displays a comparison of the load-deformation curves obtained on unreinforced and reinforced masonry walls. The results show that with the external application of textile reinforced render on one side of the masonry walls it was possible to achieve up to 5 times more load than without reinforcement. However, this greater load could only be achieved – by surpassing the masonry flexural strength – when the deformation in the wall was sufficiently increased, so that the load could be transmitted first to the rendering layer. Once the render got fine cracks, the textile reinforcement could be activated.

Due to the different stress mechanism of the single reinforced masonry components, two successive occurring failures – in the masonry and in/on the reinforcing layer – can be distinguished. With respect to the masonry, when the masonry flexural strength is reached, either the units or the bond between unit and mortar can fail. Especially in the case of walls with unfilled head joints and units with high tensile strength, joint failure is expected. Even though the units used for these tests did not reach the supposed high tensile strength ( $\leq 0.3 \text{ N/mm}^2$ ), presumably a low bond strength between unit and mortar led to bond failure on all tested walls. To confirm this assumption, the actual bond strength should be determined. With respect to the reinforcing layer, either the bond or the textile can fail. Bond failure can occur between reinforcing layer and masonry or between render and textile. As exemplified in Figure 12, the reinforcing layer of two of the three reinforced walls failed due to a delamination between render and textile (cf. Table 5). Different to the uniaxial tensile tests on TRM specimens, it was thus not possible to reach the textile strength in the reinforcing layer of the walls subjected to flexural loading.

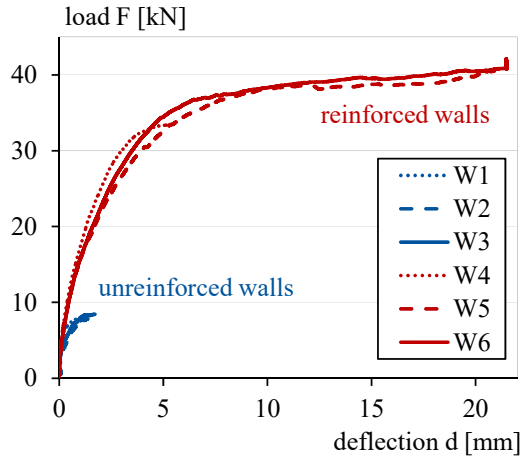


**Figure 11: Load-deformation curves of unreinforced and reinforced masonry walls under flexural load**



**Figure 12: Bond failure between render and textile of the reinforced wall w5**

Table 5 presents a summary of the walls investigated so far. Besides the materials used, the maximum measured deflections and loads  $F_{max}$ , the calculated values of the flexural strength  $f_n$  as well as the failure modes of the wall and reinforcing layer are given therein. To calculate the flexural strength a simplification with respect to the resistant moment was made, so that regardless of the reinforcement only the masonry wall resistance was taken into account. The results clearly show a substantial increase of the flexural strength of the reinforced masonry walls with respect to the unreinforced ones. Since the load transmission between the units can be improved only due to the render, further tests on rendered walls without reinforcement will be conducted. The comparison of these results with the already obtained ones will help to clarify the actual contribution of the textile in the improvement of the load-bearing capacity of masonry walls.

**Table 5: Flexural tensile tests parallel to the bed joint: series and results**

ID no.	type	head joint	unit/mortar	render/textile	$d_{max}$	$F_{max}$	$f_n$	failure mode
					mm	kN	N/mm <sup>2</sup>	
W1	un-reinforced	unfilled	U1/G2	-	1.4	8.1	0.31	j
W2					1.6	7.9	0.30	j
W3					1.7	8.4	0.32	j
W4	reinforced	unfilled	U1/G2	R1/C1	5.4	33.6	1.27	j; b <sub>1</sub>
W5					21.4	42.2	1.60	j; b <sub>2</sub>
W6					21.5	42.1	1.59	j; b <sub>2</sub>

wall: joint failure (j)  
 reinforcement: bond failure between wall and render (b<sub>1</sub>) or between textile and render (b<sub>2</sub>)

## CONCLUSIONS AND OUTLOOK

This study focuses on the analysis of the load-bearing and deformation behavior of textile reinforced masonry. In this sense and in an exemplary manner, two reinforcement textiles (AR-glass and carbon) in combination with two cement renders were investigated with regard to their bond performance under tensile load. The best bond performance was obtained with an

impregnated carbon textile (C1) combined with a cement render free from additives (R1). In this case, the textile utilization degree was 60-80 % in waft and weft direction. In the second part of the research project this material combination was used to reinforce one surface of the clay masonry walls subjected to flexural loading. The test results clearly demonstrate the effectiveness of in cement rendering embedded carbon textile for improving the flexural load resistance of masonry. In total, up to 5 times higher flexural strength values parallel to the bed joint were achieved with textile reinforced masonry compared to unreinforced masonry.

However, the study does not make clear yet to what extent the render and to what extent the textile contribute to increase the masonry flexural load resistance. Neither is known what would be the improvement if a bond failure between the reinforcing materials did not occur, but a textile failure. Future research will try to clarify this. To generalize the analysis, further investigations will include other reinforcing materials combined with other masonry units and mortar types.

## REFERENCES

- [1] Scheerer, S.; Schladitz, F. and Curbach M. (2015), "Textile reinforced concrete – from the idea to a high performance material." Bagnex: RILEM. FERRO-11 *Proc., 11th International Symposium and 3rd ICTRC International Conference on Textile Reinforced Concrete, Aachen, Germany 7-10 June 2015*, (Bramshuber, W. (Ed.)), 15-34
- [2] Saenger, D. and Bramshuber, W. (2015) "Reinforced masonry using textiles." Bagnex: RILEM. FERRO-11. *Proc., 11th International Symposium and 3rd ICTRC International Conference on Textile Reinforced Concrete, Aachen, Germany, 7-10 June 2015*, (Bramshuber, W. (Ed.)), 511-521
- [3] Saenger, D. and Bramshuber, W. (2016). "Bond Behaviour between Textile and Mortar for Masonry Strengthening." Boca Raton [u.a.]: CRC Press, 2016. *Proc., 16th International Brick and Block Masonry Conference, Padova, Italy, 26-30 June 2016*, 425-431, ISBN 978-1-138-02999-6
- [4] Bramshuber, W. (2016). "RILEM TC 232-TDT: Recommendation of RILEM TC 232-TDT: Test Methods and Design of Textile Reinforced Concrete. Uniaxial Tensile Test: Test Method to Determine the Load Bearing Behavior of Tensile Specimens Made of Textile Reinforced Concrete." *Materials and Structures*, RILEM 49, Nr. 12, 4923-4927
- [5] Scholzen, A. Chudoba, R. and Hegger, J. (2015), "Ultimate limit state assessment of TRC shell structures with combined normal and bending loading." Bagnex: RILEM. FERRO-11 *Proc., 11th International Symposium and 3rd ICTRC International Conference on Textile Reinforced Concrete, Aachen, Germany, 7-10 June 2015*, (Bramshuber, W. (Ed.)), 159-166